Original Article

JCBFM

Journal of Cerebral Blood Flow & Metabolism
2020, Vol. 40(6) 1316–1327

DOI: 10.1177/0271678X19861448
journals.sagepub.com/home/jcbfm
SAGE

The functional role of hemojuvelin in acute ischemic stroke

Guang-Huar Young[1], Sung-Chun Tang[2], Vin-Cent Wu[3], Kuo-Chuan Wang[4], Jing-Yi Nong[3], Po-Yuan Huang[2], Chaur-Jong Hu[5], Hung-Yi Chiou[6], Jiann-Shing Jeng[2] and Chung Y Hsu[7]

Abstract

Our study aimed to establish the role of hemojuvelin (HJV) in acute ischemic stroke (AIS). We performed immunohistochemistry for HJV expression in human brain tissues from 10 AIS and 2 non-stroke autopsy subjects. Plasma HJV was measured in 112 AIS patients within 48 h after stroke. The results showed significantly increased HJV expression in brain tissues from AIS patients compare to non-stroke subjects. After adjusting for clinical variables, plasma levels of HJV within 48 h after stroke were an independent predictor of poor functional outcome three months post-stroke (OR:1.78, 95% CI: 1.03–3.07; $P = 0.038$). In basic part, Western blotting showed that HJV expression in mice brains was apparent at 3 h after middle cerebral artery occlusion (MCAO), and increased significantly at 72 h. In cultured cortical neurons, expression of HJV protein increased remarkably 24 h after oxygen glucose deprivation (OGD), and small interfering RNAs (siHJV) transfected OGD neurons had a lower apoptotic rate. Importantly, 72 h post-MCAO, HJV knockout mice had significantly smaller infarcts and less expression of cleaved caspase-3 protein compared with wild-type mice. In summary, HJV participates in the mechanisms of post-stroke neuronal injury, and that plasma HJV levels can be a potential early outcome indicator for AIS patients.

Keywords

Acute ischemic stroke, hemojuvelin protein, neuron, iron, outcome

Received 1 February 2019; Accepted 17 May 2019

Introduction

Stroke is among the three leading causes of death worldwide and is the most frequent cause of permanent disability.[1] Epidemiological studies have shown that ischemic stroke accounts for approximately 75%–85% of all strokes.[2] Currently, acute recanalization, either via intravenous thrombolytic therapy or intra-arterial thrombectomy, is the most effective treatment for acute ischemic stroke (AIS).[3] However, few AIS patients currently receive recanalization therapy and, of those who do, not all have good functional outcomes.[4] Thus, it is important to investigate the mechanisms involved in post-AIS neuronal damage and to look for novel potential therapeutic targets.

Results from previous studies have suggested that the breakdown of blood–brain barriers (BBBs) subjected to red blood cells causes deposition of hemoglobin-derived neurotoxic iron.[5] The hemoglobin-derived iron from cerebral brain injury may be involved in the generation of reactive oxygen species (ROS) by the catabolism of Haber–Weiss and Fenton reactions.[1] Increased free radicals that are catalyzed by free iron

[1]Division of Scientific Research, Energenesis Biomedical, Taipei
[2]Stroke Center and Department of Neurology, National Taiwan University Hospital, Taipei
[3]Department of Internal Medicine, National Taiwan University Hospital, Taipei
[4]Department of Surgery, National Taiwan University Hospital, Taipei
[5]Department of Neurology, Taipei Medical University-Shuang Ho Hospital, Taipei
[6]School of Public Health, Taipei Medical University, Taipei
[7]Graduate Institute of Clinical Medical Science, China Medical University, Taichung

Corresponding author:
Sung-Chun Tang, Department of Neurology, National Taiwan University Hospital, No.7 Chung-Shan South Road, Taipei 100.
Email: sctang@ntuh.gov.tw

have been demonstrated in several experimental models of stroke.[6] Furthermore, various iron chelators have been shown to reduce the associated injury.[7,8]

Systemic iron homeostasis is controlled by the hemojuvelin (HJV)-hepcidin-ferroportin axis in the liver,[9] and upstream HJV exists in intact membrane-bound and proteolytic forms, which work reciprocally in response to iron status.[10] In spite of most studies reported that the major source of HJV in plasma originates in skeletal muscle,[11] skeletal muscle HJV is dispensable for systemic iron homeostasis.[12,13] Several studies have provided evidence that HJV is increased in the kidney in response to ischemic renal injury, and proteolytic HJV was validated prospectively in plasma and urine as a biomarker for acute kidney injury.[14,15]

Recent research has shown that the protein hepcidin plays a role in AIS. Its possible mechanism involves down-regulating ferroportin in ischemic brain to regulate iron levels.[16–18] However, the role of HJV during acute ischemic brain injury is still unclear, even when HJV protein has been detected in numerous organs, such as the liver, heart, kidney, brain, and in muscle tissue.[19,20]

To better define the role of HJV during AIS, we evaluated in the brain and plasma following clinical stroke, in the brain following experimental stroke in mice, and in cultured neurons to oxygen–glucose deprivation (OGD) treatment (modeling ischemia in vitro).

Materials and methods

Human brain tissue

Human brain tissue samples were obtained from 2 anonymous autopsy non-stroke subjects and 10 AIS patients receiving decompressive craniectomy and lobectomy for large hemispheric infarction at National Taiwan University Hospital. The clinical parameters of AIS patients are shown in Supplementary Table 1. The brain tissues were collected soon after the patients died or surgery. Samples were taken mainly from the temporal lobe within the infarct area in AIS patients. The human brain staining protocol was approved from the National Taiwan University Hospital Ethics Committee. Brain specimens were fixed in 4% buffered formalin for at least three weeks before paraffin embedding. Brain sections were processed for immunofluorescence staining or IHC with a non-biotin-amplified method (Novocastra Laboratories Ltd, Newcastle Upon Tyne, UK) using primary antibodies against human HJV (Abnova). Slides were analyzed using TCS SP8 confocal microscopy (Leica-Microsystems, Mannheim, Germany). Cell percentage of HJV positive, HO-1 positive, and occludin positive for each biopsy specimen were analyzed and compared between stroke patients and controls.

Clinical study

We designed a multicenter trial of AIS patients at one medical center (National Taiwan University Hospital) and two regional hospitals (National Taiwan University Hospital, Yun-Lin Branch, and Taipei Medical University-Shuang Ho Hospital). This study was approved by the ethics committees of the National Taiwan University Hospital (NTUH) Ethics Committee and Institutional Review Board of Taipei Medical University (TMU) and conducted in accordance with ethical standards of the responsible committee in NTUH and TMU on human experimentation. All patients gave written informed consent.

Between 2009 and 2015, patients with AIS who were admitted within 24 h and had received the first blood draw within 48 h after onset were recruited per our established standard protocol.[21,22] The diagnosis of AIS was confirmed by magnetic resonance imaging (diffusion-weighted image) or repeated computed tomographic exams (performed $\geq$ 24 h after stroke onset to clearly demonstrate the infarct region).[23] Etiologic subtypes of AIS were determined based on the Trial of Org 10172 in Acute Stroke Treatment (TOAST) criteria, including large artery atherosclerosis, small vessel occlusion, cardio-embolism, stroke of other determined etiologies, and stroke of undetermined etiology.[24] Patients were excluded if they had active infection, autoimmune disease, or cancer. Those who were unable to receive two time points of blood drawing after stroke or unwilling to receive post stroke follow-up were also excluded.

Blood samples were drawn at within 48 h after the onset of stroke. A detailed history of the clinical presentation, vascular risk factors, and comorbidity was obtained for each patient. Stroke severity at admission was assessed by the National Institutes of Health Stroke Scale (NIHSS). Mortality and functional outcome three months after stroke onset were determined. Good outcome was defined as a modified Rankin Scale (mRS) score $\leq$ 2. In our study, NIHSS was evaluated by the primary physician and recorded on the medical chart. mRS at three months post stroke was evaluated by the study nurses of participating hospitals who were not involved in the presented study and blinded to the blood testing results.

Human plasma collection and measurements

A 10-mL sample of blood was drawn from IS patients into an EDTA tube, then centrifuged at 300*g* for 15 minutes, aliquoted into 1.5-mL tubes, and stored

at −80°C until used.[25,26] The plasma levels of HJV were determined using a commercially ELISA kit (Wuhan USCN Business Co., Wuhan, China) according to the manufacturer's protocol. This ELISA kit has been reported for the measurement of HJV from clinical samples in previous studies.[14,15] Samples with obvious hemolysis, which was visually detected by showing a pinkish-red tinge inside, were not used for measurements.

Animals

All animal protocols and procedures were approved by the National Taiwan University College of Medicine Institutional Animal Care and Use Committee (IACUC Approval No: 20140439). All mice were housed in standard 12-h light dark cycle with free access to food and water. All experiments in this study adhered to the ARRIVE guidelines for animal experiments. Ten to 12 weeks-old of male wild-type C57BL/6 mice and 129S mice were purchased from Lasco Co., Ltd (Taiwan), and HJV knockout mice (129S-Hfe2^{tm1Nca}/J) were purchased from the Jackson Laboratory (Bar Harbor, ME) and maintained on an inbred 129S6/SvEvTac background.[27]

Cell cultures and OGD model

Dissociated cell neuron-enriched cultures of cerebral cortex were established from E15-day mouse embryos. Cells were plated in 60-mm-diameter plastic or 35-mm glass-bottom dishes on a polyethyleneimine substrate in 0.8 mL of medium consisting of Minimum Essential Medium Eagle with Earle's salts, supplemented 10% with heat-inactivated fetal bovine serum (FBS) (Gibco, Grand Island, NY, USA)/1 mM L-glutamine/1 mM pyruvate/20 mM KCl/26 mM sodium bicarbonate (pH 7.2). Following cell attachment, the culture medium was replaced with Neurobasal Medium with B27 supplements (Gibco). Experiments were performed in seven- to nine-day-old cultures.[28] Approximately 95% of the cells in such cultures were neurons, and the remaining cells were astrocytes. For OGD treatment, neurons were washed with glucose-free Hanks' balanced salt solution (HBSS), incubated in glucose-free Locke's medium and then transferred to an oxygen-free chamber containing 95% N2 and 5% CO2 atmosphere for 1 or 3 h. Then the medium was replaced with neurobasal medium (Gibco), and the cells were incubated under usual culture conditions for 24, 48, or 72 h.

Middle cerebral artery occlusion and reperfusion

Briefly, mice were anesthetized with isoflurane, a midline incision was made in the animal's neck, and the left external carotid and pterygopalatine arteries were isolated and ligated with 6–0 silk thread. The internal carotid artery (ICA) was occluded at the peripheral site of the bifurcation of the ICA, and the pterygopalatine artery with a small clip and the common carotid artery (CCA) were ligated with 5–0 silk thread. The external carotid artery (ECA) was cut, and 6–0 nylon monofilament with a blunted tip (0.2–0.22 mm) with a coagulator was inserted into the ECA. After the clip at the ICA was removed, the nylon thread was advanced into the middle cerebral artery (MCA) until light resistance was felt. The nylon thread and the CCA ligature were removed after 1 h of occlusion, to initiate reperfusion. In a sham group, these arteries were visualized but not disturbed. After 72 h of reperfusion, the mice were sacrificed by the following procedure: Mice were exposed to concentration of isoflurane over 5%. After the breathings of mice were stop, continue exposure for additional 1 min. The mice brains were immediately removed and placed into PBS (4°C) for 15 min. Four 2-mm coronal sections were made from the olfactory bulb to the cerebellum. The brain sections were stained with 2% 2, 3,5-triphenyltetrazolium chloride (TTC) in phosphate buffer at 37°C for 15 min. The stained sections were photographed, and the digitized images were then analyzed. The borders of the infarct in each brain slice were outlined and the area quantified using NIH image J 6.1 software. To correct for brain swelling, the infarct area was determined by subtracting the area of undamaged tissue in the left hemisphere from that of the intact contralateral hemisphere. The final infarct area was determined by calculating the percentage of infarcted area in each brain slice. Total infarct volume was calculated by integration of infarct areas for all slices of each brain.[29] For the collection of brain tissue, the mice were sacrificed, perfused with cold PBS, decapitated, and brains were carefully removed from the skull on ice. The ischemic hemisphere containing the infarct core and penumbra regions was dissected, and then quickly immersed in liquid nitrogen and stored in −80°C prior to further analysis.

Iron quantification

The concentration of total iron in brain tissues was quantitated using inductively coupled plasma atomic emission spectroscopy (ICP-AES) as previously described.[15] Briefly, the brains from each mouse were digested with 0.5, 1.0 and 1.0 ml of mixed acid (HNO3/HC104 = 122 5:1, v/v), and the solutions were diluted with distilled water to 5, 10 and 10 ml, respectively. The concentrations of iron in these mice brains were determined simultaneously using ICP-AES (Jarrell-Ash Model 975 Plasma Atomcomp).

Western blot analysis

Cell lysates were obtained by washing the cells in ice-cold PBS and re-suspending the cell pellets in cell lysis buffer. Brain tissue was extracted using T-PER tissue protein extraction buffer containing protease and phosphatase inhibitor mixture (Visual Protein, Taipei, Taiwan). Protein concentration was determined using a BCA protein assay kit (Visual Protein).[30] Protein in samples (30 μg) was separated by sodium dodecyl sulfate polyacrylamide gel electrophoresis (SDS-PAGE) (8% to 12%) and transferred onto a PVDF membrane. The membrane was blocked in 5% BSA for 1 h at room temperature, followed by overnight incubation at 4°C with primary antibodies. The membrane was then washed and incubated with a secondary antibody for 1 h at room temperature. Protein bands were visualized by using LumiFlash Prime Chemiluminescent Substrate and recorded with a Chemlux SPX-600 Series Imager (Visual Protein).

RNA interference

siRNA against HJV (Origene Inc., Valencia, CA) was complexed with lipofectamine® RNAiMAX (Invitrogen, Carlsbad, CA) reagent according to the manufacturers' protocols.[31] In brief, 1 μL lipofectamine and 10 pmol siRNA was mixed in 50 μL of Opti-MEM I (Gibco) and then added into 1×10^4 primary neurons/well. After 6 h of transfection, the medium was replaced by cultural medium for an additional 18 h before OGD treatment. The knockdown efficiency was confirmed by Western blot analysis from another batch of siRNA-treated neuronal cells.

Cell viability assay

Cell viability was determined by the cell counting kit-8 (CCK-8) (Dojindo Molecular Technologies, Kumamoto, Japan). Briefly, cells were seeded in 96-well plates at 1×10^4 primary neurons/well and transfected with siRNA. After OGD treatment, 10 μL of CCK-8 reagent was added and the plates were then incubated for 2 h in CO_2 incubator. The absorbance was measured at 450 nm using a microplate reader.[32]

Immunocytochemistry

Primary neurons were grown on 25-mm microscope coverslips and fixed in 4% paraformaldehyde for 20 min. After washing, the coverslips were blocked in PBS containing 10% FCS and 0.1% Triton X-100, incubated at room temperature for 1 h with mice monoclonal or polyclonal anti-HJV antibodies (Abnova, Taipei, Taiwan), followed by a 1-h incubation with Alexa Fluor 488-conjugated specific secondary antibodies (Invitrogen) at room temperature.[33] Images of cells were acquired using LSM 510 confocal microscopy (Carl Zeiss AG, Oberkochen, Germany).

Immunohistochemistry

The murine brains were fixed in 4% formaldehyde in PBS (freshly prepared from paraformaldehyde powder) overnight at 4°C before being transferred to sequential 20% and 30% solutions of sucrose (wt/vol) at 4°C until the brains sank to the bottom of the solution. The brains were then embedded in Sakura® TissueTek™ (Sakura) before sectioning (10-μm sections were made using a cryostat) in the coronal anatomic plane.[34] Sections were first exposed for a minimum of 30 min to PBS containing 0.1% Triton X-100 (Amresco, Radnor, PA) and 10% normal goat serum (Jackson ImmunoResearch Laboratories Ltd, Pennsylvania, USA) to block nonspecific antibody binding, followed by incubation overnight with the relevant primary antibodies. Sections were then washed and incubated for 1 h in the presence of appropriate secondary antibodies. Images were acquired using LSM 510 confocal microscopy (Carl Zeiss AG, Oberkochen, Germany).

Statistics

Statistical analyses were performed using SPSS version 18.0 software (SPSS Inc., Chicago, IL). Experimental results are expressed as the mean ± SD, and comparisons between the data sets were performed by non-parametric Mann–Whitney U or Kruskall–Wallis tests (SPSS & GraphPad Prism 6; GraphPad Software, La Jolla, CA). In the clinical study, due to no previous study regarding the HJV in stroke for reference, we used the previous studies related to the levels of HJV in patients with acute kidney injury, and cardiovascular surgery as well as our previous stroke biomarkers studies for the sample estimation and decided to recruit around 100 study subjects.[14,15,22,25] Besides, subjects were excluded with any missing value of main clinical variables for the multivariable analysis. The differences in the clinical and biochemical parameters between good and poor functional outcomes were analyzed using the Chi-square test, and the two-sample *t*-test in univariate analysis. In the multivariable analysis, a logistic regression method was used to adjust with age and sex and those with univariable P values of <0.05, including hypertension, diabetes mellitus, and NIHSS at admission. Significance was defined as $P < 0.05$.

Results

HJV was elevated in human brains after AIS

We compared the expression of HJV in a non-stroke autopsy subjects ($n=2$) and an AIS patient ($n=10$) by immunostaining (Figure 1 and Supplementary Figure 1). Figure 1(a) shows the positive immunohistochemical staining of HJV from cortical region of stroke patient and non-stroke control, but with much less signal intensity in the latter. The localization of HJV in the stroke patient brain sections was found in cells with positive staining of neuronal marker against anti-MAP2 but minor in cells staining with microglia marker against anti-IBA1 (Figure 1(b)). Furthermore, previous studies showed that the inducible HO-1 is a promising marker to estimate oxidative stress in neuron after AIS.[35] The co-localization staining of HJV and HO-1 from cortical region revealed a significantly higher percentage of positive expression of HJV and HO-1 in acute stroke patients than non-stroke controls (Figure 1(c) and (d)). These brain tissues from patients in reference to the infarction region were schematized with red

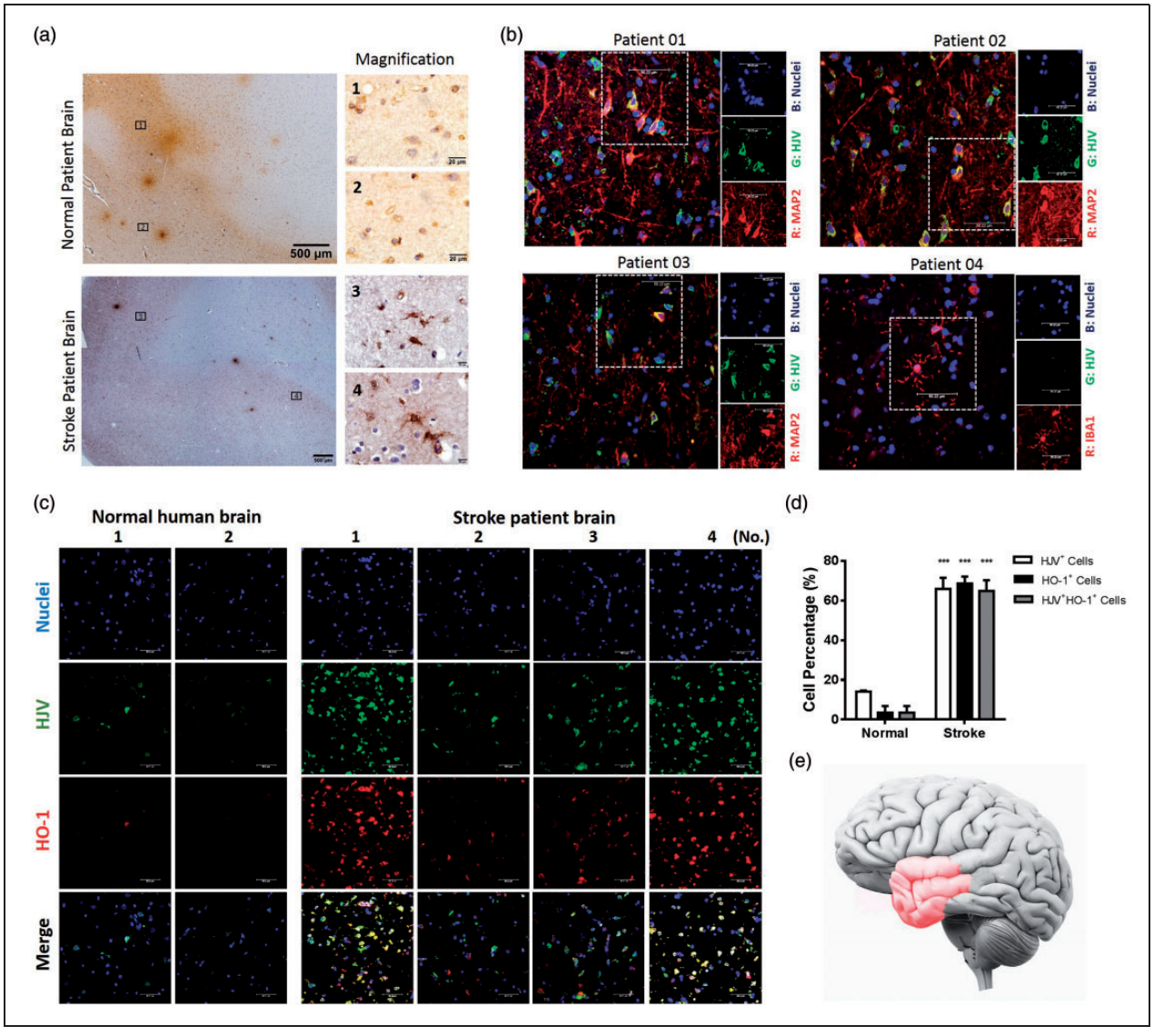

Figure 1. Cells immunoreactive to HJV were found in human brain tissues and were more abundant in stroke patients ($n=10$) than controls ($n=2$). (a) Immunohistochemical staining of HJV from cortex region of normal ($n=2$) and acute stroke patient ($n=10$). (b) Characterization of cells expressing HJV in the stroke patient brain section ($n=4$) by double immunofluorescence with anti-MAP2 or anti-IBA1 antibodies. (c) Double immunofluorescence micrographs of HJV and HO-1 from cortex region of normal ($n=2$) and acute stroke patients ($n=4$). Scale bars: 50 μm. (d) Percentage of HJV-positive cells, HO-1-positive cells or double-positive cells among total cells from biopsy specimen. Data were expressed as mean±SD; ***, $P<0.001$ vs. control group. (e) Schematic of the clinical human brain tissue in reference to the infarction region (Red color).

color in Figure 2(e). To characterize the relation of BBB breakdown with HJV, we assessed the integrity of a tight junction-associated protein in microvessels of patient brain section. Here we used the transmembrane protein occlidin, which represented as the biomarker for severe BBB damage.[36,37] Compared with the normal patients, the reduction and discontinuity of occludin along the cerebral microvessels were observed in brain tissue from stroke patients (Supplementary Figure 2).

Plasma HJV is a prognostic indicator of poor AIS outcome

Of 112 AIS patients (mean age: 66.5 ± 12.9 years, 67.9% male), 37 (33%) had poor functional outcome three months post-stroke. Patients with poor functional outcome were older, higher NIH Stroke Scale score, higher frequencies of diabetes mellitus, and hypertension, and higher plasma levels of HJV (<48 h after stroke), as compared to those with poor functional outcome (all: $P < 0.05$) (Table 1). Importantly, after adjustment for clinical variables including age, sex, hypertension, diabetes mellitus, and NIHSS at admission, plasma levels of HJV within 48 h after stroke remained an independent indicator of poor prognosis three months post-stroke (odds ratio: 1.78, 95% confidence interval: 1.03–3.07; $P = 0.038$). Stroke patients were divided into three groups of outcome as normal to mild (mRS 0–2, $n = 37$), moderate (3–4, $n = 42$) and severe (5–6, $n = 33$) functional disabilities and generated a

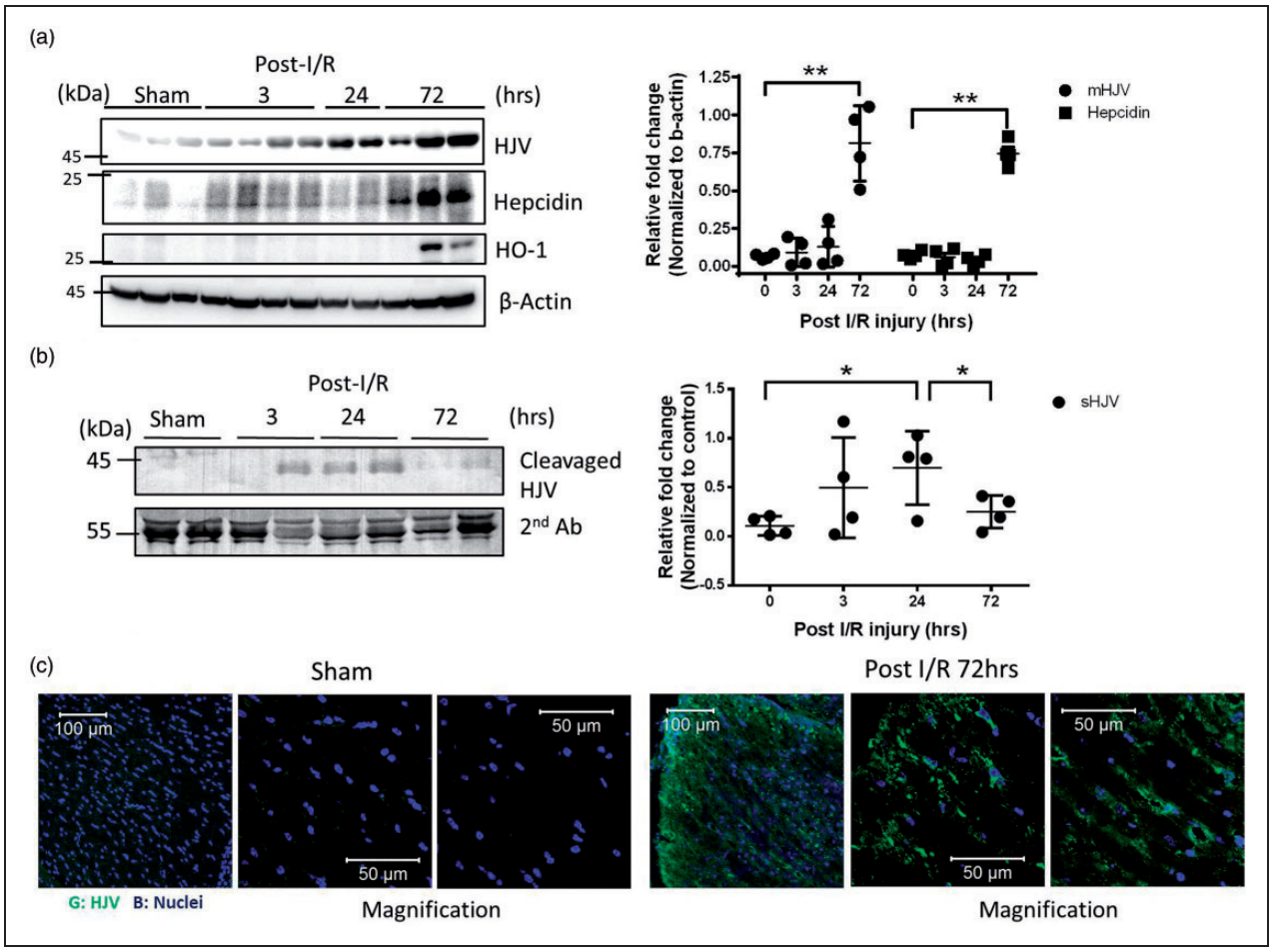

Figure 2. Time-course of HJV/Hepcidin axis in mice after receiving middle cerebral artery occlusion. (a) Brains of stroke mice were dissected at 3, 24, 72 h after MCAO surgery and compared with sham group. Representative Western immunoblots for HJV, Hepcidin, and HO-1 in mice brain at indicated time point. Quantification of immunoblot band intensity of brain lysates for each time point. Intensities of bands were normalized by β-actin, which was used as loading controls. $n = 7$ in sham, post-I/R 3, or 72 h group. $n = 6$ in post-I/R 24 h group. (b) Bloods from stroke mice after immunoprecipitation with HJV antibody were analyzed by immunoblotting. Intensities of bands were normalized by anti-mice serum, which was used as loading control. Molecular size markers are indicated at the left in kDa. Data were expressed as mean±SD; *, $P < 0.05$; **, $P < 0.01$ versus sham group. (c) Immunofluorescence staining of HJV in mice brain sections revealed significantly increased HJV expression in Mice brains from C57BL/6 mice suffered 1 h MCAO surgery and 72 h reperfusion ($n = 2$ in each group).

Table 1. Comparison by functional outcome for patients with acute ischemic stroke.

	mRS ≤ 2[a] ($n=37$)	mRS >2 ($n=75$)	*P*-value
Age, year	61.0 ± 12.0	69.2 ± 12.6	***0.001***
Male	27 (73.0)	49 (65.3)	0.520
Initial SBP (mmHg)	164.3 ± 30.5	156.6 ± 36.1	0.279
Initial DBP (mmHg)	94.5 ± 17.8	90.1 ± 22.1	0.302
Initial HR	85.5 ± 18.4	78.4 ± 22.5	0.109
Diabetes mellitus	8 (21.6)	37 (49.3)	***0.007***
Hypertension	25 (67.6)	67 (89.3)	***0.008***
Hyperlipidemia	17 (45.9)	34 (45.3)	0.784
Atrial fibrillation	17 (45.9)	39 (52.0)	0.688
Smoking	14 (37.28)	29 (38.7)	1.000
History of stroke	11 (29.7)	23 (30.7)	1.000
Hemoglobin, g/dL	14.3 ± 1.8	14.1 ± 2.2	0.595
Glucose, mg/dL	126.2 ± 38.4	136.5 ± 46.3	0.249
Creatinin, mg/dL	1.2 ± 1.0	1.3 ± 1.1	0.475
TOAST			0.216
LAA	4 (10.8)	13 (17.3)	
CE	15 (40.5)	38 (50.6)	
Others	18 (48.6)	24 (30.8)	
NIHSS (IQR)	8 (4–14)	17 (12–20)	***<0.001***
HJV <48 h (mg/dL)	1.28 ± 0.85	2.36 ± 2.64	***0.017***

Note: Values are number (percentage), mean±standard deviation, or median. IQR: interquartile range; mRS: modified Rankin scale; NIHSS: National Institute of Health Stroke Scale; LAA: large artery atherosclerosis; CE: cardioembolism; Others, small vessel occlusion, other determined and undetermined etiologies. [a]Unfavorable outcome is mRS >2 at three months after stroke. P-value <0.05 was labeled as bold and italic number.

scatterplot based on each individual's plasma HJV level and functional outcome. As shown in the Supplementary Figure 3, stroke patients with outcomes of moderate or severe functional disability had significantly higher levels of plasma HJV levels than those with normal to mild functional disability ($P < 00.5$).

HJV expression is increased in mice brains after ischemic injury

We performed a time-course of Western analysis to determine the HJV protein levels in mice brain receiving MCAO surgery. As shown in Figure 2(a), the protein expression of HJV was low in basal conditions in mice brains. After MCAO surgery, HJV was noted early, 3 h postoperatively, and significantly elevated at 72 h, compared with expression among the sham group ($P < 0.01$). Similarly, the appearance of downstream protein-hepcidin was also detected at the same time with HJV at 72 h after MCAO compared with the sham group ($P < 0.01$). The specificity of anti-HJV antibodies was validated by recombinant HJV protein and tissues from HJV knockout mice by Western analysis (Supplementary Figure 4). To clarify the oxidative state of mice brain receiving MCAO surgery, haem oxygenase-1 (HO-1) was used to compare with time-course of HJV expression. Western analysis revealed that HO-1 was induced in mice brain significantly at 72 h after MCAO surgery (Figure 2(a)). In the same experiment, immunoprecipitation of HJV from mice plasma revealed that the cleavage form of HJV can be detected at 3 h and significantly increased at 24 h compared with measurements from the sham group. This declined at 72 h after MCAO surgery (Figure 2(b)).

Consistent with Western analysis from mice brain tissue, immunofluorescence staining showed that the expression of HJV was elevated significantly in the cerebral cortex of an ischemic mouse brain 72 h after MCAO surgery compared to a brain in the sham control group (Figure 2(c)).

Levels of HJV expression in murine primary neuron following OGD

Primary neurons were subjected to 1-h OGD and cells were returned to culture medium and incubated in the presence of oxygen to mimic the reperfusion for various time points (24, 48, and 72 h). As shown in Figure 3(a), immunofluorescence staining revealed that HJV protein was elevated following OGD in neurons. To identify the role of HJV in ischemic neuronal injury, siRNA specifically targeted to HJV was transfected to cultures of primary neurons after OGD. In Figure 3(b), CCK-8 results showed that cell exposed to 1 h OGD made a decrease on cell viability, whereas HJV siRNA did not harm cell survival in the same condition. Although the knockdown of HJV may attenuate the neuronal death following 1 h OGD treatment, once neuron cell exposed to a longer time (OGD 3 h), the OGD resulted in cell death was irreversible.

Since the JNK signaling pathway is associated with post ischemic neuron apoptosis,[38] we compared the correlation among phosphorylated JNK and HJV in OGD neuron by Western analysis. Figure 3(c) shows that OGD and re-oxygenation upregulated the levels of HJV and the phosphorylated c-Jun N-terminal kinase (P-JNK) antibody in a time-dependent manner, whereas cells transfected with siRNA to knockdown the expression of HJV did not elevate the phosphorylation of JNK (Figure 3(d)).

HJV knockout mice had a better outcome than did wild-type mice after MCAO surgery

To elucidate the functional role of HJV in acute stroke, MCAO surgery was performed in HJV knockout and

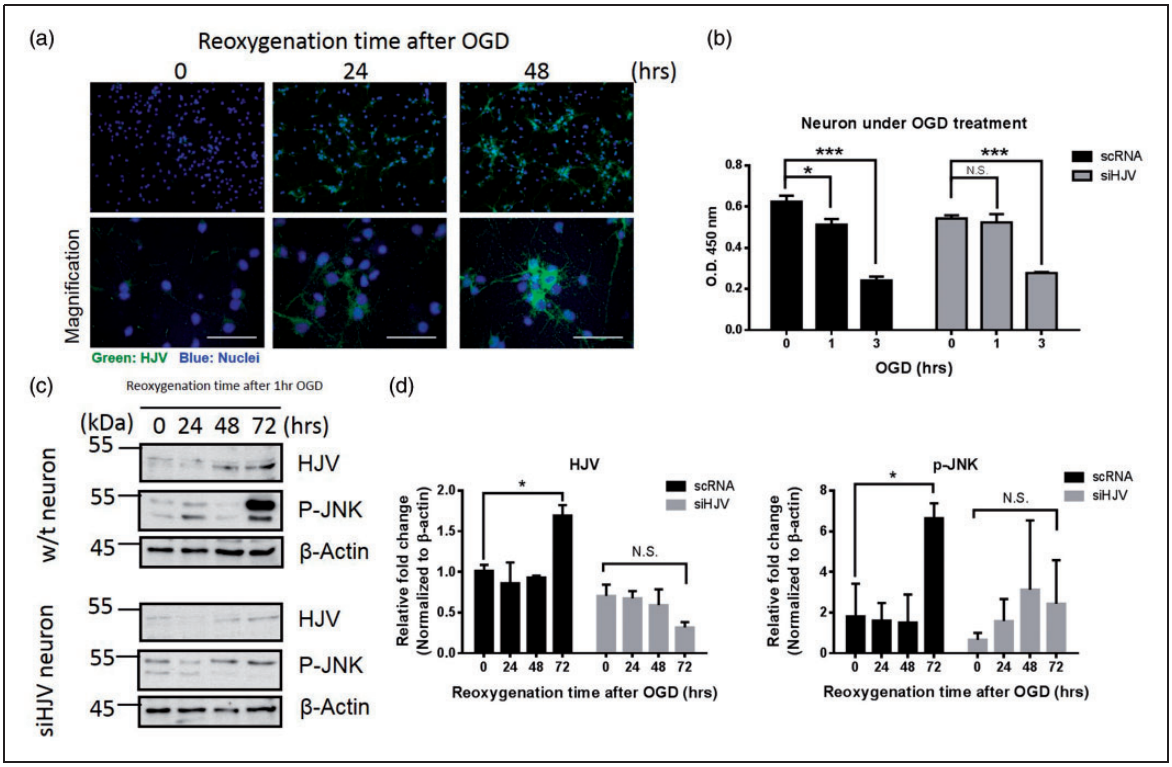

Figure 3. HJV was increased in mice neuron cells under OGD condition. (a) Mice neuron cells under OGD for different time points. Cells were fixed and stained with anti-HJV (green) and DPAI (blue). Scale bars: 50 μm. (b) Cell viability of mice neuron cells was performed by CCK-8 method. Cells transfected with scRNA or siHJV to knockdown the expression of HJV under OGD treatment at a designated time point. (c) Representative Western immunoblots for HJV and phosphorylated JNK from mice neuron cells under reoxygenation condition at indicated time point after OGD treatment. (d) Intensities of bands were normalized by β-actin, which was used as loading control. Molecular size markers were indicated at the left in kDa. Data were expressed as mean ± SD, $n = 3$. *$P < 0.05$; ***, $P < 0.001$; N.S., no significant versus control group.

wild-type mice. As shown in Figure 4(a) and (b), TTC stain revealed that HJV knockout mice had significantly reduced infarct volume than wild-type control mice after 1-h MCAO surgery and 72-hour reperfusion ($8.0 \pm 2.4\%$ vs. $43.2 \pm 2.5\%$; $n = 7$ in each group; $P < 0.01$). We next examined whether mice's lack of HJV could affect the expression of downstream target hepcidin after MCAO surgery. Western blot analysis showed hepcidin in the ischemic section was elevated after MCAO surgery, both in wild-type and HJV knockout mice (Figure 4(c)). However, the elevated level of hepcidin in response to ischemic stroke in wild-type mice was significant than in HJV knockout mice (Figure 4(d), 0.9 ± 0.3 vs. 0.45 ± 0.2; $n = 7$ in wild-type and $n = 7$ in $HJV^{-/-}$ mice; $P < 0.05$). In addition, cleaved caspase 3 protein in mice brain after MCAO surgery was much less significant in HJV knockout mice compared with wild-type mice (Figure 4(d), 0.34 ± 0.06 vs. 0.78 ± 0.12; $n = 7$ in wild-type and $n = 7$ in $HJV^{-/-}$ mice; $P < 0.05$).

Discussion

HJV is a multifaceted protein that plays distinct roles for iron homeostasis in many organs.[39–41] Mutations in HJV lead to blunt hepcidin expression, resulting in iron overload, as in juvenile hemochromatosis.[42,43] In spite of most studies reported that the major source of HJV in plasma originates in skeletal muscle,[11] skeletal muscle HJV is dispensable for systemic iron homeostasis.[12,13] Our data showed that the expression of HJV is extra low in mice brain in basal conditions. After an acute stroke, we detected the elevation of HJV protein, which exists in membrane form in brain tissue and as the cleavage form in plasma. We speculated that the increased HJV in plasma might originate from leakage of the intrinsic pathway due to the damage of BBB after stroke and from an extrinsic reaction from skeletal muscle or liver in response to acute systemic stress after stroke.

During AIS, iron released from broken red blood cells was deposited into neurons, leading to more

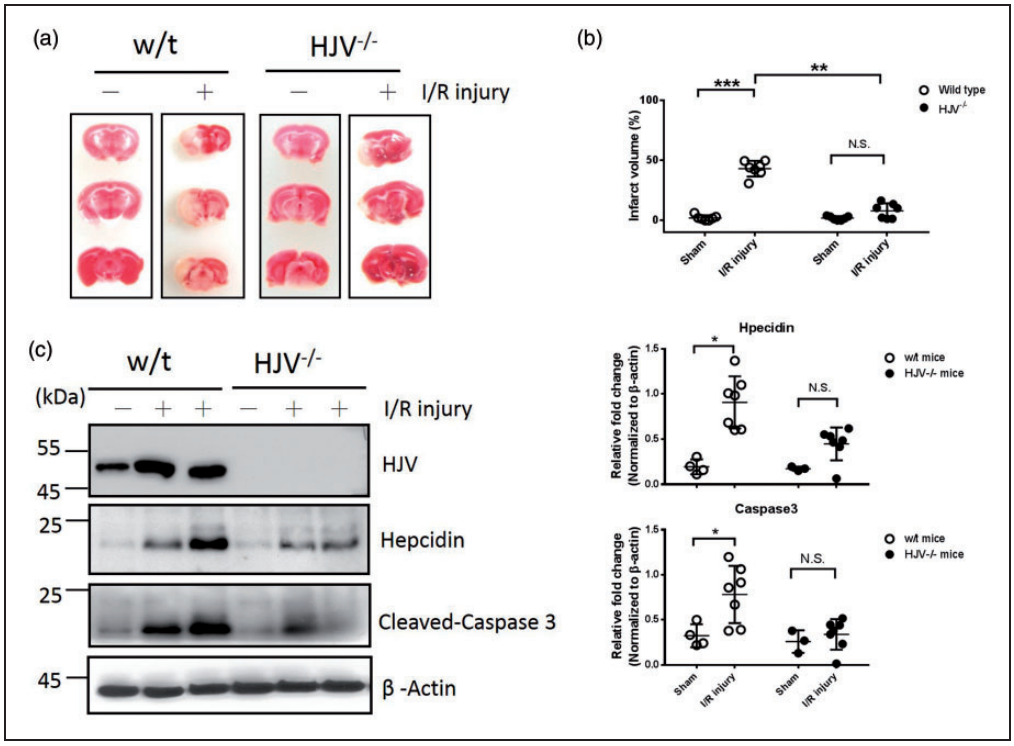

Figure 4. The effect of ischemic outcomes in wild-type and HJV knockout mice. Mice receiving 1 h MCAO surgery and 72 h reperfusion. (a) Representative pictures of TTC-stained brain sections in wild-type and HJV knockout mice. (b) Infarct volume in mice. Data were expressed as mean±SD, $n = 7$ in each group; **, $P < 0.01$; ***, $P < 0.001$; N.S., no significant versus sham-operated group. (c) Representative Western immunoblots for HJV, Hepcidin, cleaved-caspase 3 in mice brain. (d) Intensities of bands were normalized by β-actin, which was used as loading control. Molecular size markers are indicated at the left in kDa. In sham group, $n = 4$ in wild-type and $n = 3$ in $HJV^{-/-}$ mice. In post I/R group, $n = 7$ in wild-type and $n = 7$ in $HJV^{-/-}$ mice. Data were expressed as mean±SD, *, $P < 0.05$; N.S: no significant.

serious oxidative stress.[44,45] We know that ferroportin is the sole iron exporter to expel excess iron from BBB into the circulation.[46] Upregulation of serum hepcidin is associated with downregulation of ferroportin in brain.[47] Degradation of ferroportin in BBB blunted the iron efflux from brain into plasma during acute stroke.[48] This explains why the brain damage is ameliorated in hepcidin knockdown mice and exogenous hepcidin is worse during ischemic injury.[48] Interestingly, the elevation of hepcidin in mice brains has been shown associated with inflammation, iron overload, and ischemic damage,[28,42,49] and the origins of hepcidin in ischemic brain are mainly from astrocyte and microglia.[48] Our results showed that HJV was elevated in neuron cells after OGD process, but we did not observe the expression of hepcidin in OGD neurons (Data not shown). Using HJV knockout mice, hepcidin was also minor elevation in the ischemic cortex compared to wild-type mice. Therefore, we speculated that the elevation of HJV may be partially independent on the regulation of hepcidin, even though both were up-regulated in ischemic brain. Although previous studies have shown that ischemic/reperfusion injury result in iron deposition in mice brain,[16] we did not detect the significant difference of brain iron content among wild type and HJV knockout mice after stroke (Supplementary Figure 5). This let us rethink about the non-iron-related functions of HJV in mice brain.

In our study, neuronal apoptosis in the ischemic cortex investigated by infarct size and caspase-3 immunostaining was both ameliorated in HJV knockout mice as compared with wild-type mice. Furthermore, the cell viability assay and alleviated phosphorylated JNK (P-JNK) immunostaining results in siHJV transfected neurons had a lower apoptotic rate than control neurons under the OGD process. These results indicated that increased HJV is involved in stroke injury through the enhancement of apoptotic reactions in the ischemic cortex. Thus, HJV may be a target for the treatment of stroke.

Many studies showed that the neuroprotective function of transforming growth factor beta (TGF-β) is

induced following a variety of types of brain tissue injury,[50] and TGF-β-mediated signaling could attenuate cell apoptosis.[51] In another study, the expression of TGF-β in the liver of naïve HJV knockout uncovered higher levels than wild type mice.[52] The direct interaction between HJV and TGF-β on skeletal muscle was observed in recently published muscle-wasting models by muscle-specific HJV knockout mice, and HJV is a suppressor to inhibit TGF-βs signaling in cell membrane.[53] Correspondingly, our result using HJV knockout mice and siHJV neuron has identified the negative correlation between HJV and TGF-β in vivo and in vitro (Supplementary Figure 6). The basal levels of TGF-β in siHJV mice neuron and HJV knockout mice are not merely higher than control groups, and the elevations of TGF-β are also far above than control groups which receive OGD or stroke treatment. Whether do the additional elevation of TGF-β in $HJV^{-}/^{-}$ stroke mice and siHJV neuron in OGD attenuate the cell apoptosis? Future studies are warranted to better understand the precise mechanism of HJV after stroke caused TGF-β signaling.

Not only did our study clarify the biophysiological mechanisms of post-stroke neuronal injury, the results also suggested that HJV plasma level could be an early prognostic indicator after AIS. The present study collected plasma at two time points within three days after stroke, and the first sample was obtained within 48 h AIS. This indicates that early time point of plasma levels of HJV may reflect the severity of ischemic brain injury. The expression pattern and prognostic potential for the plasma HJV in our AIS patients was similarity reflected in the results from our experimental stroke research. Whether the circulating HJV in plasma behaves as a biomarker only or directly participates in post-stroke brain injury deserves further investigation. Nevertheless, our study did provide comprehensive basic and clinical evidence for the direct involvement of HJV-mediated signaling in AIS.

Our study had several limitations. First, there is a lack of information about the association of iron and HJV, because we did not prospectively monitor the effect of iron deposition on the duration of stroke. Future studies, with more accurate iron quantification, are warranted. Second, plasma HJV in AIS patients cannot be specially clarified into central or systemic origin. In the future, more extensive studies with conditionally labeled HJV may provide valuable information on this issue. Third, although we demonstrated the independently detrimental effect of plasma HJV in AIS, it is difficult to establish and verify a clinically useful cutoff value indicating poor functional outcome in AIS patients. Further studies with larger sample sizes will be needed to strengthen our findings.

Conclusions

HJV may play a critical role in response to stroke injury through apoptotic reactions. Disruption of HJV ameliorates neuronal death and brain damage, thus reducing infarct size after focal ischemic stroke. Our clinical data also suggested that plasma levels of HJV are positively correlated with poor post-stroke outcome. Additional research is required to better understand the underlying mechanisms of HJV in AIS.

Funding

The author(s) disclosed receipt of the following financial support for the research, authorship, and/or publication of this article: This work was supported by the Ministry of Science and Technology. Grants (104-2628-B-002-004) and the Ministry of Health and Welfare, Taiwan (MOHW107-TDU-B-212-123004), China Medical University Hospital, Academia Sinica Taiwan Biobank, Stroke Biosignature Project (BM10701010021), NRPB Stroke Clinical Trial Consortium (MOST 106-2321-B-039-005-).

Acknowledgements

We are thankful for the support of the 3rd core facility at the National Taiwan University Hospital and Spectral Confocal Laser Scanning Platform Laboratory in department of Life Science, Fu-Jen Catholic University.

Declaration of conflicting interests

The author(s) declared no potential conflicts of interest with respect to the research, authorship, and/or publication of this article.

Authors' contributions

GHY, SCT, HYC, JSJ, and CYH designed research; GHY, SCT, KCW, JYN, PYH, VCW, and C J H performed research and data analysis; GHY, SCT, and JSJ wrote the paper HYC, and CYH gave the critical revision.

Supplementary material

Supplemental material for this article is available online.

References

1. Sutton HC. Efficiency of chelated iron compounds as catalysts for the Haber-Weiss reaction. *J Free Radic Biol Med* 1985; 1: 195–202.
2. Hsieh FI, Lien LM, Chen ST, et al. Get with the guidelines-stroke performance indicators: surveillance of stroke care in the Taiwan stroke registry: get with the guidelines-stroke in Taiwan. *Circulation* 2010; 122: 1116–1123.
3. Powers WJ, Rabinstein AA, Ackerson T, et al. 2018 guidelines for the early management of patients with acute ischemic stroke: a guideline for healthcare professionals from the American Heart Association/American Stroke Association. *Stroke* 2018; 49: e46–e110.

4. Goyal M, Menon BK, van Zwam WH, et al. Endovascular thrombectomy after large-vessel ischaemic stroke: a meta-analysis of individual patient data from five randomised trials. *Lancet* 2016; 387: 1723–1731.
5. Keep RF, Zhou N, Xiang J, et al. Vascular disruption and blood-brain barrier dysfunction in intracerebral hemorrhage. *Fluids Barriers CNS* 2014; 11: 18.
6. Davalos A, Fernandez-Real JM, Ricart W, et al. Iron-related damage in acute ischemic stroke. *Stroke* 1994; 25: 1543–1546.
7. Xia S, Zhang W, Huang L, et al. Comparative efficacy and safety of deferoxamine, deferiprone and deferasirox on severe thalassemia: a meta-analysis of 16 randomized controlled trials. *PLoS One* 2013; 8: e82662.
8. Sorond FA, Tan CO, LaRose S, et al. Deferoxamine, cerebrovascular hemodynamics, and vascular aging: potential role for hypoxia-inducible transcription factor-1-regulated pathways. *Stroke* 2015; 46: 2576–2583.
9. Niederkofler V, Salie R and Arber S. Hemojuvelin is essential for dietary iron sensing, and its mutation leads to severe iron overload. *J Clin Invest* 2005; 115: 2180–2186.
10. Lin L, Goldberg YP and Ganz T. Competitive regulation of hepcidin mRNA by soluble and cell-associated hemojuvelin. *Blood* 2005; 106: 2884–2889.
11. Silvestri L, Pagani A and Camaschella C. Furin-mediated release of soluble hemojuvelin: a new link between hypoxia and iron homeostasis. *Blood* 2008; 111: 924–931.
12. Chen W, Huang FW, de Renshaw TB, et al. Skeletal muscle hemojuvelin is dispensable for systemic iron homeostasis. *Blood* 2011; 117: 6319–6325.
13. Gkouvatsos K, Wagner J, Papanikolaou G, et al. Conditional disruption of mouse hfe2 gene: maintenance of systemic iron homeostasis requires hepatic but not skeletal muscle hemojuvelin. *Hepatology* 2011; 54: 1800–1807.
14. Ko SW, Chi NH, Wu CH, et al. Hemojuvelin predicts acute kidney injury and poor outcomes following cardiac surgery. *Sci Rep* 2018; 8: 1938.
15. Young GH, Huang TM, Wu CH, et al. Hemojuvelin modulates iron stress during acute kidney injury: improved by furin inhibitor. *Antioxid Redox Signal* 2014; 20: 1181–1194.
16. Ding H, Yan CZ, Shi H, et al. Hepcidin is involved in iron regulation in the ischemic brain. *PLoS One* 2011; 6: e25324.
17. Shin JA, Kim YA, Kim HW, et al. Iron released from reactive microglia by noggin improves myelin repair in the ischemic brain. *Neuropharmacology* 2018; 133: 202–215.
18. Slomka A, Switonska M and Zekanowska E. Hepcidin levels are increased in patients with acute ischemic stroke: Preliminary report. *J Stroke Cerebrovasc Dis* 2015; 24: 1570–1576.
19. Rodriguez Martinez A, Niemela O and Parkkila S. Hepatic and extrahepatic expression of the new iron regulatory protein hemojuvelin. *Haematologica* 2004; 89: 1441–1445.
20. Rodriguez A, Pan P and Parkkila S. Expression studies of neogenin and its ligand hemojuvelin in mouse tissues. *J Histochem Cytochem* 2007; 55: 85–96.
21. Tang SC, Wang YC, Li YI, et al. Functional role of soluble receptor for advanced glycation end products in stroke. *Arterioscleros Thrombos Vasc Biol* 2013; 33: 585–594.
22. Tang SC, Yeh SJ, Tsai LK, et al. Cleaved but not endogenous secretory rage is associated with outcome in acute ischemic stroke. *Neurology* 2016; 86: 270–276.
23. Tang SC, Jen HI, Lin YH, et al. Complexity of heart rate variability predicts outcome in intensive care unit admitted patients with acute stroke. *J Neurol Neurosurg Psychiatry* 2015; 86: 95–100.
24. Adams HP Jr., Bendixen BH, Kappelle LJ, et al. Classification of subtype of acute ischemic stroke. Definitions for use in a multicenter clinical trial. Toast. Trial of org 10172 in acute stroke treatment. *Stroke* 1993; 24: 35–41.
25. Tang SC, Yang KC, Hu CJ, et al. Elevated plasma level of soluble form of rage in ischemic stroke patients with dementia. *Neuromol Med* 2017; 19: 579–583.
26. Lee DH, Kim JW, Jeon SY, et al. Proteomic analysis of the effect of storage temperature on human serum. *Ann Clin Lab Sci* 2010; 40: 61–70.
27. Huang FW, Pinkus JL, Pinkus GS, et al. A mouse model of juvenile hemochromatosis. *J Clin Invest* 2005; 115: 2187–2191.
28. Tang SC, Arumugam TV, Xu X, et al. Pivotal role for neuronal toll-like receptors in ischemic brain injury and functional deficits. *Proc Natl Acad Sci U S A* 2007; 104: 13798–13803.
29. Lee S, Lee M, Hong Y, et al. Middle cerebral artery occlusion methods in rat versus mouse models of transient focal cerebral ischemic stroke. *Neural Regen Res* 2014; 9: 757–758.
30. Young GH, Lin JT, Cheng YF, et al. Identification of adenine modulating ampk activation in nih/3t3 cells by proteomic approach. *J Proteomics* 2015; 120: 204–214.
31. Cheng YF, Young GH, Chiu TM, et al. Adenine supplement delays senescence in cultured human follicle dermal papilla cells. *Exp Dermatol* 2016; 25: 162–164.
32. Cheng YF, Young GH, Lin JT, et al. Activation of amp-activated protein kinase by adenine alleviates TNF-alpha-induced inflammation in human umbilical vein endothelial cells. *PLoS One* 2015; 10: e0142283.
33. Sun CY, Young GH, Hsieh YT, et al. Protein-bound uremic toxins induce tissue remodeling by targeting the EGF receptor. *J Am Soc Nephrol* 2015; 26: 281–290.
34. Wu VC, Young GH, Huang PH, et al. In acute kidney injury, indoxyl sulfate impairs human endothelial progenitor cells: modulation by statin. *Angiogenesis* 2013; 16: 609–624.
35. Wang J and Dore S. Heme oxygenase-1 exacerbates early brain injury after intracerebral haemorrhage. *Brain* 2007; 130: 1643–1652.
36. Shi S, Qi Z, Ma Q, et al. Normobaric hyperoxia reduces blood occludin fragments in rats and patients with acute ischemic stroke. *Stroke* 2017; 48: 2848–2854.

37. Pan R, Yu K, Weatherwax T, et al. Blood occludin level as a potential biomarker for early blood brain barrier damage following ischemic stroke. *Sci Rep* 2017; 7: 40331.
38. Mielke K and Herdegen T. Jnk and p38 stresskinases – degenerative effectors of signal-transduction-cascades in the nervous system. *Prog Neurobiol* 2000; 61: 45–60.
39. Przybyszewska J and Zekanowska E. The role of hepcidin and haemojuvelin in the pathogenesis of iron disorders in patients with severe malnutrition. *Ann Agric Environ Med* 2014; 21: 336–338.
40. Core AB, Canali S and Babitt JL. Hemojuvelin and bone morphogenetic protein (bmp) signaling in iron homeostasis. *Front Pharmacol* 2014; 5: 104.
41. Siebold C, Yamashita T, Monnier PP, et al. RGMs: structural insights, molecular regulation, and downstream signaling. *Trends Cell Biol* 2017; 27: 365–378.
42. Fleming RE, Feng Q and Britton RS. Knockout mouse models of iron homeostasis. *Annu Rev Nutr* 2011; 31: 117–137.
43. Ravasi G, Pelucchi S, Mariani R, et al. A severe hemojuvelin mutation leading to late onset of hfe2-hemochromatosis. *Dig Liver Dis* 2018; 50: 859–862.
44. Lipscomb DC, Gorman LG, Traystman RJ, et al. Low molecular weight iron in cerebral ischemic acidosis in vivo. *Stroke* 1998; 29: 487–492; discussion 493.
45. Lipinski B, Pretorius E, Oberholzer HM, et al. Interaction of fibrin with red blood cells: the role of iron. *Ultrastruct Pathol* 2012; 36: 79–84.
46. Coffey R and Ganz T. Iron homeostasis: an anthropocentric perspective. *J Biol Chem* 2017; 292: 12727–12734.
47. Raha-Chowdhury R, Raha AA, Forostyak S, et al. Expression and cellular localization of hepcidin mRNA and protein in normal rat brain. *BMC Neurosci* 2015; 16: 24.
48. Xiong XY, Liu L, Wang FX, et al. Toll-like receptor 4/myd88-mediated signaling of hepcidin expression causing brain iron accumulation, oxidative injury, and cognitive impairment after intracerebral hemorrhage. *Circulation* 2016; 134: 1025–1038.
49. Wang Q, Du F, Qian ZM, et al. Lipopolysaccharide induces a significant increase in expression of iron regulatory hormone hepcidin in the cortex and substantia nigra in rat brain. *Endocrinology* 2008; 149: 3920–3925.
50. Kim BH and Levison SW. Tgfbeta1: Friend or foe during recovery in encephalopathy. *Neuroscientist* 2018; 25: 192–198.
51. Yu Y, Li J, Zhou H, et al. Functional importance of the tgf-beta1/smad3 signaling pathway in oxygen-glucose-deprived (OGD) microglia and rats with cerebral ischemia. *Int J Biol Macromol* 2018; 116: 537–544.
52. Sebastiani G, Gkouvatsos K, Maffettone C, et al. Accelerated CCL4-induced liver fibrosis in $HJV^{-/-}$ mice, associated with an oxidative burst and precocious profibrogenic gene expression. *PLoS One* 2011; 6: e25138.
53. Zhang P, He J, Wang F, et al. Hemojuvelin is a novel suppressor for duchenne muscular dystrophy and age-related muscle wasting. *J Cachexia Sarcopenia Muscle* 2019; 10: 557–573.